

K-Ar Geochronology of the Survey Pass, Ambler River  
and Eastern Baird Mountains Quadrangles,  
Southwestern Brooks Range,  
Alaska

by

Donald L. Turner\*, Robert B. Forbes\*,  
and Charles F. Mayfield\*\*

U. S. Geological Survey Open-File Report  
Prepared in cooperation with the State of Alaska  
Department of Natural Resources, Division of  
Geological and Geophysical Surveys

\*Geophysical Institute and Solid-Earth Sciences Program  
University of Alaska  
Fairbanks, Alaska 99701

\*\* U. S. Geological Survey  
Menlo Park, California 94025

This report is preliminary and has  
not been edited or reviewed for  
conformity with Geological Survey  
standards and nomenclature.

## ABSTRACT

We report 76 previously unpublished K-Ar mineral ages from 47 metamorphic and igneous rocks in the southwestern Brooks Range. The pattern of radiometric ages is complex, reflecting the complex geologic history of this area. Local and regional radiometric evidence suggests that the southern Brooks Range schist belt has, at least in part, undergone a late Precambrian metamorphism and that the parent sedimentary and igneous rocks for the metamorphic rocks dated as late Precambrian are at least this old (Precambrian Z).

This schist terrane experienced a major thermal event in mid-Cretaceous time, causing widespread resetting of nearly all K-Ar mica ages. A series of apparent ages intermediate between late Precambrian and mid-Cretaceous are interpreted as indicating varying amounts of partial argon loss from older rocks during the Cretaceous event.

The schist belt is characterized by dominant metasediments and subordinate metabasites and metafelsites. Blueschists occur within the schist belt from the Chandalar quadrangle westward to the Baird Mountains quadrangle, but geologic evidence does not support the existence of a fossil subduction zone.

## INTRODUCTION

This project was begun in 1973 as a cooperative effort involving personnel from the Alaska Division of Geological and Geophysical Surveys, U.S. Geological Survey, and the Geophysical Institute of the University of Alaska. During that summer, a N-S mapping and sampling traverse across the Southern Brooks Range schist belt was completed by Forbes, Turner, Wyatt Gilbert, and John Carden with D.G.G.S. helicopter support. In 1974 Forbes and Carden completed additional field work in the Baird Mountains quadrangle with D.G.G.S. helicopter support.

Laboratory work for K-Ar dating was supported by the D.G.G.S. and the National Science Foundation (NSF Grant GA 43004). Additional samples for dating were provided by the D.G.G.S. and U.S.G.S. from the collections of J. Fritts, R. Garland, G. Eakins, G. Pessel, I. Tailleux, W. Brosge, C. F. Mayfield and M. Wiltse. The final preparation of this report was supported by the U.S.G.S.

The report is divided into three principal parts, a section on the petrology and structural setting of the metamorphic rocks by R. B. Forbes; a section on radiometric dating by D. L. Turner; and a section on evidence for the age of metamorphism from the stratigraphic record by C. F. Mayfield.

A total of 76 new K-Ar mineral ages from 47 different metamorphic and igneous rock samples in the southwestern Brooks Range are reported. Radiometric dating was done at the Geochronology Laboratory of the Geophysical Institute, University of Alaska, Fairbanks. Analytical techniques have been reported previously (Turner and others, 1973). Analytical data for age determinations are given in Table 2. Data for previously published U.S.G.S. K-Ar ages in the area are given in Table 3.

Sample locations, along with ages and mineral symbols, are shown on Plates 1-3.

All of the dated samples come from the schist belt and nearby granitic plutons which crop out over a distance of more than 600 km along the southern flank of the Brooks Range (Beikman and Lathram, 1976). Data presented here come from the western and central parts of this schist belt in the Baird Mountains, Ambler River and Survey Pass quadrangles.

## PETROLOGY AND STRUCTURAL SETTING

### Geologic Characteristics of the Schist Belt:

The central and western segments of the southwestern Brooks Range schist belt are characterized by dominant metasediments and subordinate metabasites and metafelsites. The parent terrane was apparently composed of argillaceous and quartzose sedimentary rocks, with intercalated carbonates, basalts and felsic volcanic rocks. The belt was recrystallized under conditions of the blueschist, greenschist and lower amphibolite facies. In some areas the terrane appears to be a two-sided metamorphic belt, with highest metamorphic grade displayed by rocks along the axial zone. In other areas, however, metamorphic grade increases to the north where the effects of synkinematic recrystallization are overprinted by thermal aureoles associated with the emplacement of granitic plutons. Along some segments of the belt, including the Walker Lake and Kiana areas, the north flank of the schist terrane is concealed by allochthonous carbonates.

### Blueschist and Greenschist Metamorphism

Blueschists have been found within the schist terrane from the Chandalar quadrangle westward to the Ambler River and Baird Mountains quadrangles. As presently mapped, most of the blueschists occur as discontinuous zones or large boudin-like masses derived from parental mafic volcanic and intrusive masses. However, a few examples of chloritoid- and jadeite-bearing blueschists have been discovered, which are clearly of metasedimentary origin.

Whole-rock chemical analyses show that there is no significant difference in the sodium content of analyzed blueschists, compared to

greenschists in other parts of the schist terrane. In some cases the compositionally-analogous greenschists are retrograded blueschists. However, some of these greenschists are transitional to epidote amphibolites in prograde sections within the terrane. Additionally, sodic amphiboles occur in schists with a sodium content as low as 0.97 wt. %. The evidence clearly indicates that the presence of sodic amphibole in the metabasites is due to the high pressure/low temperature regime of blueschist facies metamorphism rather than high sodium content.

Whole-rock sodium concentrations of Brooks Range blueschists and greenschists are similar to those in metabasites from other Alaskan metamorphic terranes, with the exception of the highly sodic crossite-epidote schists in the Seldovia-Kodiak terranes which were derived from parental spillites (J. Carden, University of Alaska Ph.D. dissertation, in preparation).

Petrofabric studies of the metabasites (blueschists, greenschists and epidote amphibolites) indicate a polymetamorphic history involving a later greenschist facies thermal event which overprinted the earlier blueschists, amphibolites and eclogites (?) with imperfectly developed greenschist mineral assemblages. This event has had a pervasive effect on the apparent  $^{40}\text{K}/^{40}\text{Ar}$  mineral ages, as discussed in the following sections. Metasediments derived from argillaceous and quartzose sediments show little evidence of the later greenschist facies thermal event because the constituent mineral assemblages tend to be stable under both blueschist and greenschist facies P/T conditions.  $^{40}\text{K}/^{40}\text{Ar}$  dating, however, shows that the micas and amphiboles in these rocks have frequently been partially or totally reset by a later thermal pulse.

The earlier metamorphic event appears to have been under conditions of the low temperature sub-division of the blueschist facies (Taylor and Coleman, 1968), based on the occurrence of coarse relict jadeite in a metawacke collected from the cirque 1/4 mile east of VABM Ruby, and as metacrysts in a metabasite which crops out on the southern tip of the ridge which forms the divide between the Kogoluktuk and Mauneluk Rivers. Significantly, the jadeitic metacrysts are rimmed by secondary sodic amphibole which probably formed during the waning stages of blueschist facies metamorphism.

Additional support for a pervasive blueschist facies metamorphic event is given by the general absence of biotite in pelitic schists and metabasites in this segment of the schist belt. Notable exceptions are the biotite-bearing assemblages of the felsic schists ("button schists") which are highly potassic and have whole-rock compositions analogous to rhyolites or potassic granites, and biotite which is in contact thermal aureoles around granitic plutons north of the Walker Lake Fault. The origin of the constituent biotite and the genesis of the "button schists" is controversial. Biotite and muscovite from these schists give Cretaceous  $^{40}\text{K}/^{40}\text{Ar}$  ages, apparently produced by the pervasive Cretaceous age overprint discussed in the following section.

The absence of lawsonite and aragonite in the blueschists is no doubt due to the retrograde effects of the late greenschist facies thermal event, which has inverted the former aragonite to calcite, and promoted reactions between lawsonite and other minerals to produce clinozoisite and epidote. Petrographic evidence for these reactions includes biaxial calcite with relict optic angles up to  $40^\circ$ , and discordant clinozoisite-paragonite fabrics which are believed to be related to

retrograded lawsonite.

Initial results of oxygen isotope ( $^{18}\text{O}/^{16}\text{O}$ ) analyses by James O'Neil (personal communication) indicate that quartz-glaucophane mineral pairs were not equilibrated, whereas quartz-mica pairs from the same rocks give crystallization temperatures of 500°-600°C which would correlate with conditions of the upper greenschist facies. In addition to documenting the validity of subsequent greenschist facies metamorphism, these data are compatible with the survival of coarse-grained glaucophane in the polymetamorphic fabrics; and with the inherited argon problem associated with the dating of some of the coarse-grained glaucophanes discussed in a following section.

### Structure

The most pronounced and easily recognized structure in this part of the schist belt is an anticlinally folded nappe-like structure (Figure 1) which was first called the Kalurivik Arch (Pessel and others, 1973). The axis of this structure is 5 km north of VABM Ruby. The arch is defined by the deformation of  $S_1$  surfaces, but  $S_2$  surfaces were apparently synchronous with the development of the antiform. The arching may be related to the emplacement of the Redstone, Shishsakshinovik and Mt. Igipak-Arrigetch Peaks plutons, because these plutons are elongate parallel to the axis of the arch and have gneissic margins (Plate 2).

The Walker Lake Fault (Figure 1) was first described by Fritts (1972). Fritts believed that he could trace the fault for 100 km along the strike of the schist belt, and that it separated two distinctive terranes. The north block is characterized by low grade metasediments containing the assemblage quartz-albite-muscovite-chlorite (+ calcite,

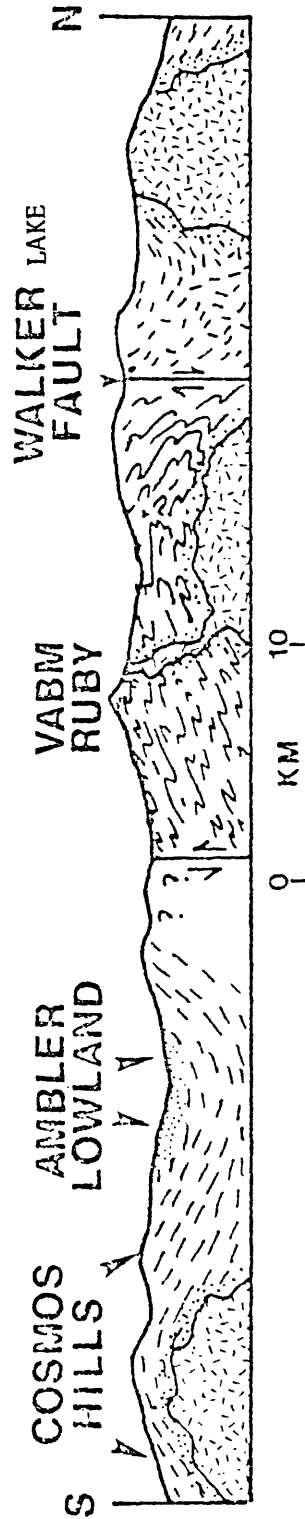


Figure 1. Generalized North-South cross section from the Cosmos Hills to the Walker Fault, Ambler River quadrangle.

biotite). In several cases, biotite appears to be incipient and to be forming from the reaction of chlorite and white mica, and not due to post-kinematic upgrading from the thermal effects of plutons. Metabasites are volumetrically less important in the north block, and to date blueschists have not been found north of the fault. This fault is controversial because it is difficult to map in some areas, and the discordance in the structure of the opposing blocks is not obvious in most areas. The fault, if real, appears to pre-date the deformation of the Kalurivik Arch, and may be a folded unconformity that has been subsequently metamorphosed.

The discovery of jadeitic pyroxene in the above described metabasite is important, as it supports the contention of Forbes and others (1974) that the metabasites and metasediments on the southern tip of the ridges between the Ambler and Kogoluktuk Rivers represent the feebly recrystallized portion of the blueschist terrane to the north, rather than a separate Devonian terrane similar to that south of the Ambler Lowland, which apparently underwent blueschist facies metamorphism at a later time (I. L. Tailleux, personal communication).

The blueschists of the schist belt are not closely associated with an ophiolite terrane, and do not appear to be related to a fossil subduction zone in their present tectonic setting. Chemical analyses of the metabasites indicate that the terrane does not include spilitic basalts, although some of the analyses are similar to those of low potassium tholeiites. Undersaturated alkali basalt analogs are missing from the mafic igneous suite.

Some of the large boudin-like masses of blueschist contain relict igneous fabrics similar to coarse-grained diabase, diorite and gabbro.

These fabrics indicate that the parent mafic igneous rocks were probably intruded as small plutons, dikes or sills. Although the bulk chemistry of these rocks is similar to continental tholeiites and basaltic andesites, the geologic evidence does not support an island arc setting.

Although the consuming plate margin is a convenient model for the generation of blueschist facies pressure-temperature conditions, there does not appear to be any evidence for a fossil subduction zone with a partially consumed oceanic plate in the areas we have studied. A plate collision model may be more appropriate for the blueschists of the southwestern Brooks Range.

## RADIOMETRIC DATING

The southwestern Brooks Range schist belt has had a complex geologic history and the K-Ar ages reflect this complex history, as can be seen from Figure 2, a histogram showing apparent ages grouped in 10 m.y. increments. Individual apparent ages range from 86 to 756 m.y.; with the dominant group in the 100-140 m.y. interval, some in the late Precambrian, and a number of ages scattered between these two extremes.

### Cretaceous Ages

The majority of the K-Ar data are from micas that yielded Cretaceous ages, and these ages are distributed throughout the 300 km length of the schist belt we have studied. We believe that the Cretaceous age grouping represents the time at which the rocks of the schist belt cooled to argon retention temperatures for muscovite and biotite following a thermal event in mid-Cretaceous time. This thermal event was pervasive throughout the entire schist terrane and may have been caused by the intrusion of the E-W-trending series of granitic plutons (Redstone, Shishakshinovik, Igipak, etc.) which core the southern part of the range (Plates 1-3). The Cretaceous age data are discussed in more detail in the following section.

In the Baird Mountains quadrangle, a small granitic pluton intruding the schist belt yielded a muscovite age of 104 and a biotite age of 94 m.y. Four schist samples distributed over a 30 km distance yielded mica ages of 98-122 m.y. (Plate 1). Also, a tuff in Cretaceous conglomerate on the Kobuk River near the southeastern corner of the quadrangle was dated by Patton and Miller (1968) at 83 m.y., indicating the presence of volcanic activity in this area in Cretaceous time.

# BROOKS RANGE AGE HISTOGRAM

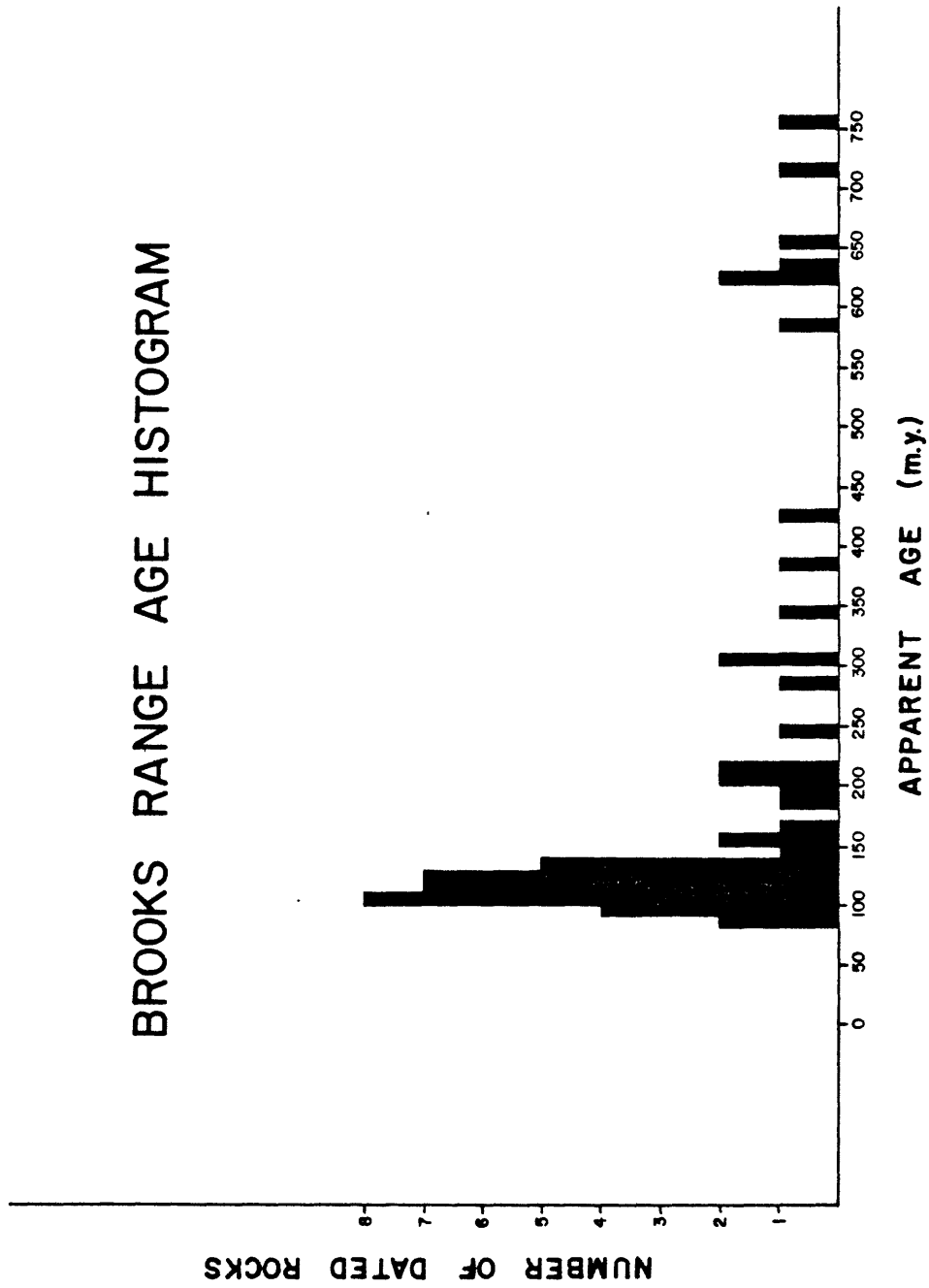


Figure 2

In the Ambler River quadrangle (Plate 2), we have dated muscovite and biotite from the southeastern contact zone of the Shishakshinovik pluton at 98 and 94 m.y., respectively. Muscovite from the core of this pluton has been dated at 99 m.y.

Within the schist belt itself, our data come from near Arctic Camp and from Ruby Ridge, the next major ridge to the west. At Arctic Camp, four schist samples collected along a 3.2 km traverse give biotite and muscovite ages of 102-117 m.y. The northernmost dating locality near Arctic Camp, however, gives a muscovite age of 160 m.y., suggesting that this particular sample did not lose all of its pre-existing argon during the Cretaceous thermal event. A small, elongate granitic body just north of the schist belt near the eastern border of the quadrangle yielded a biotite age of 86 m.y. and a muscovite age of 113 m.y.

On Ruby Ridge, four schist samples collected along a 3.2 km traverse also give biotite and muscovite ages ranging from 102 to 129 m.y., reflecting the Cretaceous event, but paragonites from three glaucophane-paragonite rocks nearby range from 213 to 234 m.y., again suggesting incomplete age resetting by the Cretaceous event. It is interesting to note that the only paragonite dated from the Baird Mountains quadrangle gives a very similar age - 191 m.y., supporting the hypothesis of incomplete argon degassing by the Cretaceous event.

In the Survey Pass quadrangle (Plate 3), Brosge and Reiser (1971) reported three mica dates from the Arrigetch Peaks Pluton ranging from 86 to 92 m.y. We obtained a 90 m.y. biotite age from this body, northeast of Walker Lake. A very small granitic pluton intruding the schist belt in the southwestern part of the quadrangle yielded biotite and muscovite ages of 100 and 115 m.y., respectively. Within the schist

belt itself we have determined 8 mica ages from schists ranging from 96 to 136 m.y.

In summary, the regional picture for the three quadrangles studied is that of a belt of granitic plutons trending E-W immediately north of the schist belt; with two much smaller granitic bodies yielding similar Cretaceous apparent ages and apparently intruding the schist belt itself. Nearly all mica ages scattered along the 300 km length of the schist belt studied yield ages in the 100 - 130 m.y. range, indicating a pervasive thermal event that cooled to argon retention temperatures for micas in mid-Cretaceous time. A few of the dated mica samples give significantly higher ages, suggesting that they were not completely reset by the Cretaceous event. Geologic evidence suggests that the Cretaceous event reflected by the K-Ar data may be a late stage of the Brooks Range late Mesozoic orogeny, as discussed in the section of this report entitled "Evidence of Regional Metamorphism from the Stratigraphic Record."

#### Late Precambrian Ages

We now wish to discuss a body of radiometric evidence which bears on the complex and controversial problem of the pre-Cretaceous metamorphic history of the Brooks Range schist belt. It is important to emphasize that this schist belt is composed of polymetamorphic rocks. These rocks have preserved evidence of a blueschist facies metamorphic event in metasediments, as well as in metaigneous rocks. Following the blueschist metamorphism, the rocks of the schist belt were retrograded in part to greenschist facies, but relict blue amphiboles are preserved in many localities scattered along the schist belt (J. Carden, University of Alaska, Ph.D. dissertation, in progress).

Unfortunately, petrologic studies cannot tell us how much time has elapsed between the formation of blue amphiboles under high pressure-low

temperature conditions and the later partial retrograding to greenschist facies at higher temperature.

The age histogram (Figure 2) shows a group of seven ages ranging from 587 to 756 m.y. These ages come from two widely separated areas in the schist belt -- four localities in the eastern Baird Mountains quadrangle and two localities from the Ruby Ridge area in the Ambler River quadrangle (Plates 1 and 2). Table 1 lists rock types, minerals dated,  $K_2O$  contents and apparent ages for these samples. Complete analytical data are given in Table 2.

These data suggest that we are looking at a schist terrane which has metamorphosed previously in late Precambrian time. The Precambrian ages come mostly from amphiboles -- the class of mineral which is most resistant to argon loss due to thermal overprinting. It should also be noted that these old ages are present in mineral having an extreme range of potassium content (from as low as 0.035%  $K_2O$  in one of the glaucophanes to 0.74% in the hornblende and up to 9.35% in the muscovite).

In a high pressure-low temperature blueschist environment, one might expect a problem with inherited argon -- that is, argon degassed from the parent rocks and occluded within the recrystallizing minerals during metamorphism. This would be a particular problem for low-potassium minerals such as glaucophanes, where a given amount of inherited argon could have a very large effect on the calculated apparent age.

And, in fact, there are five glaucophane schists from Ruby Ridge which appear to be strongly affected by this problem -- their apparent ages range from 1.3 to 2.6 billion years (Plate 2, Table 2). These apparent ages are clearly erroneous due to inherited argon, as will be discussed below. They have been omitted from Figure 2 and Table 1

TABLE 1

SOUTHERN BROOKS RANGE SCHIST BELT METAMORPHIC MINERAL AGES  
PLOTING ON 634 M.Y. ISOCHRON

| Field Number                      | Rock Type      | Mineral     | K <sub>2</sub> O<br>(Wt. %) | Age |
|-----------------------------------|----------------|-------------|-----------------------------|-----|
| <u>Baird Mountains Quadrangle</u> |                |             |                             |     |
| 74AF 144-3                        | Amph. Schist   | Actinolite  | 0.091                       | 622 |
| 74ATr 129.7                       | Actin. Schist  | Actinolite  | 0.088                       | 651 |
| 74AF 155-13                       | Glauc. Schist  | Glaucophane | 0.052                       | 756 |
| 74AF 145-5                        | Amph. Schist   | Hornblende  | 0.74                        | 719 |
| 74AF 145-1                        | Musc. Schist*  | Muscovite   | 9.35                        | 636 |
| <u>Ambler River Quadrangle</u>    |                |             |                             |     |
| 73RR7G                            | Glauc. Schist* | Glaucophane | 0.038                       | 587 |
| 73RR52                            | Glauc. Schist  | Glaucophane | 0.035                       | 630 |
|                                   |                |             | $\bar{X}_7 = 657 \pm 60$    |     |

\* Metasedimentary rocks; others are metaigneous

because they have no geologic significance.

The problem then is to distinguish between geologically meaningful ages and those which are anomalously old due to inherited argon. This can be done in two ways:

1. By examining the potassium content of each mineral yielding a Precambrian apparent age in Tables 1 and 2, one sees that it is not only the minerals with very low  $K_2O$  contents that have Precambrian ages. These ages come from minerals whose  $K_2O$  contents vary from 0.035 to 9.35%  $K_2O$ , as discussed above. If all of the late Precambrian ages were erroneous and caused by inherited argon, the grouping of seven similar ages from minerals having such an extreme (267:1) range of  $K_2O$  content -- the glaucophanes, actinolite, hornblende, blue-green amphibole and muscovite shown in Table 1 -- would be highly improbable, if not impossible.

2. Another way to approach this problem is to analyze the data using an  $^{40}Ar$  radiogenic/ $^{40}K$  isochron diagram. This type of diagram is a plot of apparent radiogenic  $^{40}Ar$  against  $^{40}K$ , on cartesian coordinates. Ideally, for a suite of coeval samples, the isochron is a straight line with the y-axis intercept being the initial  $^{40}Ar$  content of each mineral at the time the K-Ar clock was set; i.e., how much inherited argon, if any, is present. The slope is a function of geologic age.

Figures 3 and 4 are isochron diagrams plotted at two different scales to illustrate different features of the data. The Precambrian ages are seen to define a straight line (isochron) whose slope gives the late Precambrian age of 634 m.y. Twelve separate mineral analyses are plotted on this diagram (Figure 3): eight glaucophanes, one blue-green amphibole, one actinolite, one hornblende and one muscovite. All are from the schist belt and all are from schists having mineral assemblages that represent the same P-T metamorphic recrystallization event.

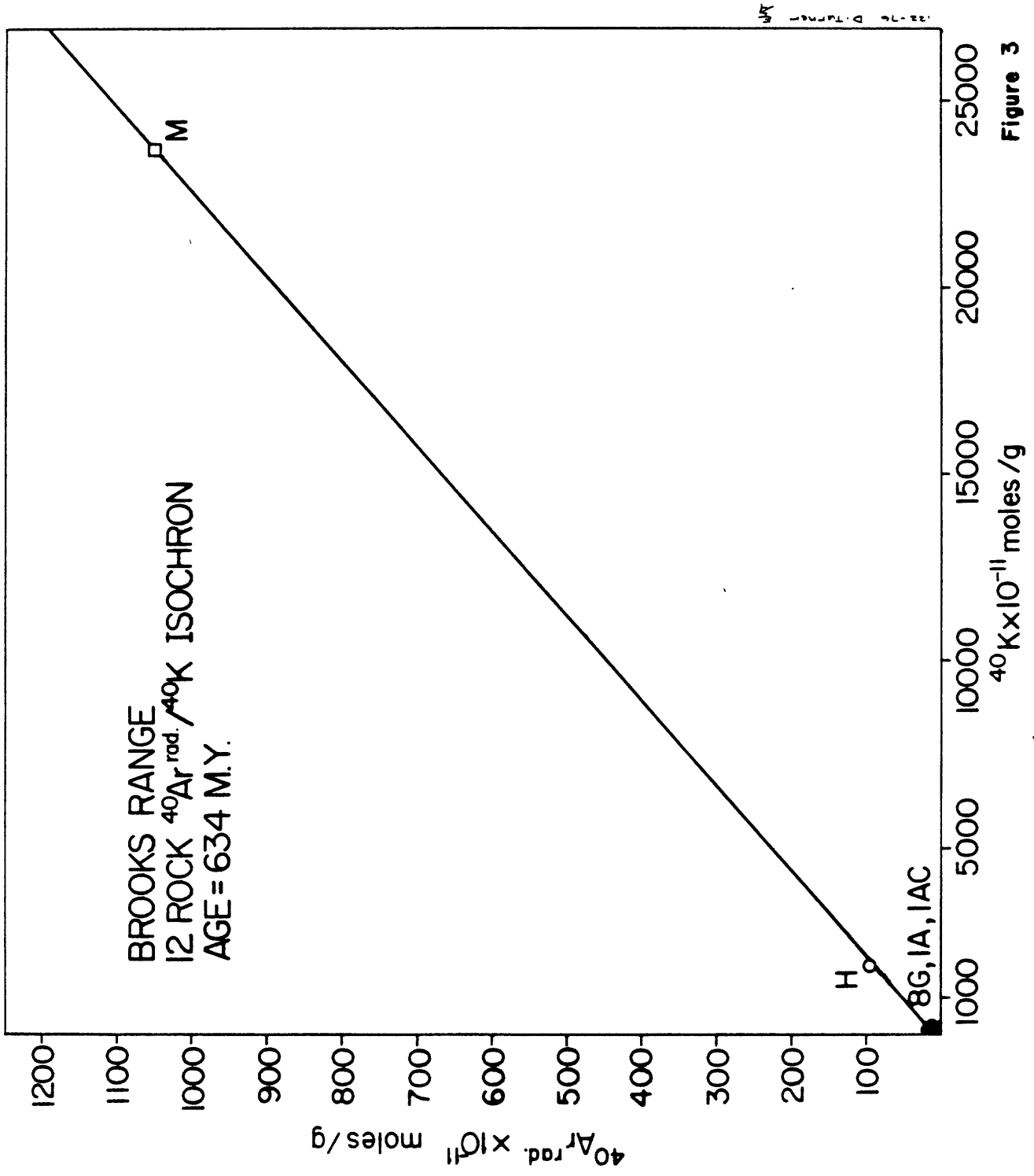
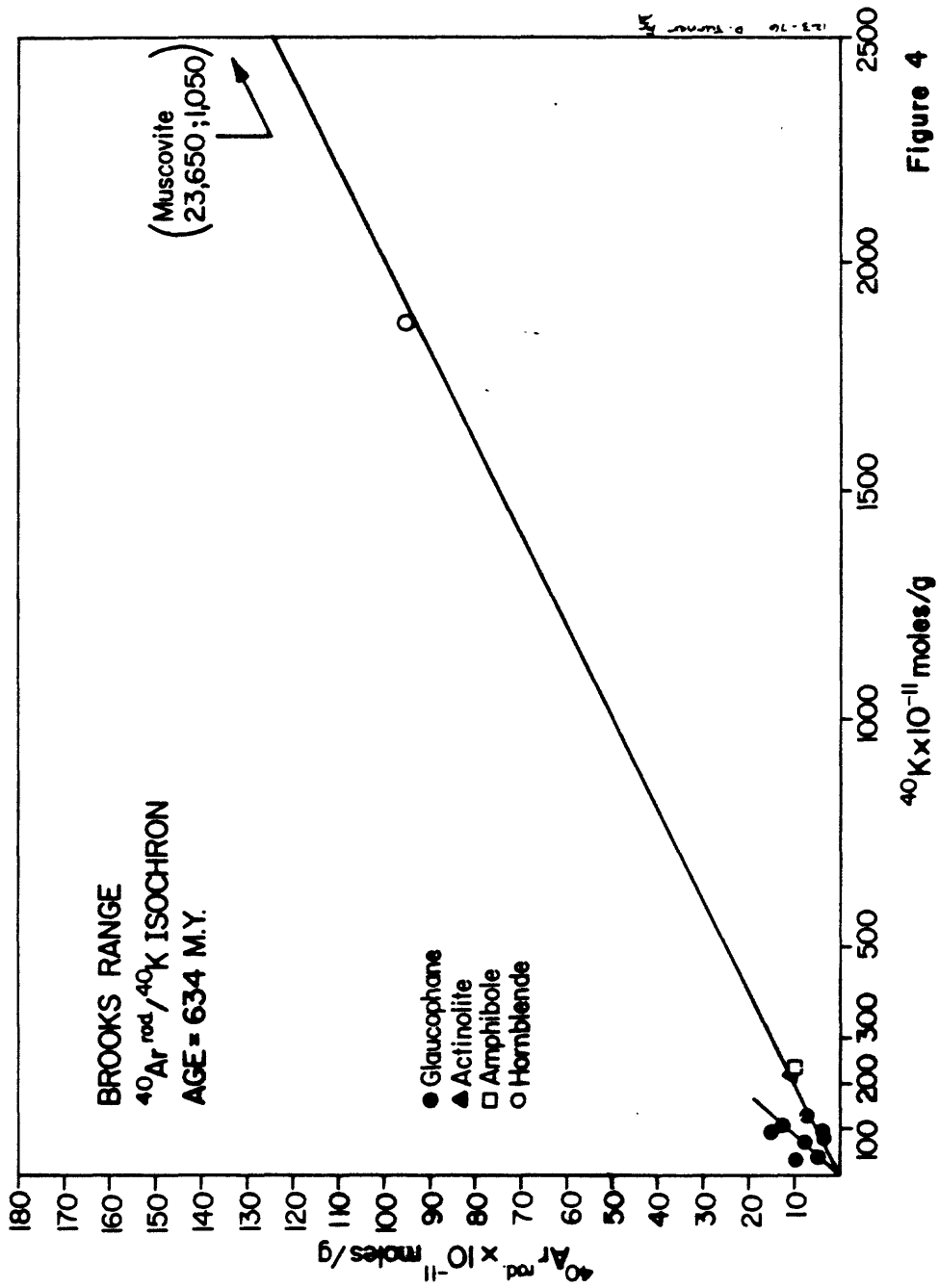


Figure 3



**Figure 4**

Strictly speaking, the use of an isochron analysis of these data may be questioned, because of the implicit assumption that all of the plotted minerals contained non-radiogenic argon of the same isotopic composition at the time of metamorphic recrystallization. It is highly unlikely (but not impossible) that such a condition would occur in different rocks scattered at considerable distances along a regional metamorphic belt.

We believe, however, that plotting these data graphically on an isochron diagram is a useful exercise which may help to illustrate some of the features of the argon system we are dealing with, as follows:

1. Five of the individual glaucophane apparent ages from the Ruby Ridge area plot significantly above the isochron when the scale is expanded sufficiently to show the fine structure of the data near the origin (Figure 4). This shows that the assumption discussed above is not true for the system as a whole. These five glaucophanes apparently contain varying but significant amounts of inherited argon, that is,  $^{40}\text{Ar}$  which was occluded in the individual minerals at the time of their formation in response to a partial pressure of  $^{40}\text{Ar}$  in the system during metamorphic recrystallization. Because the potassium content of these glaucophanes is extremely low, a relatively small amount of inherited argon can have a very large effect on the calculated apparent K-Ar age, and apparent ages of these samples range from 1.3 to 2.5 b.y. The glaucophane ages which are believed to have been significantly increased by inherited argon are preceded by asterisks in Table 2 and on Plates 1-3.

At the outset of this study, when only four glaucophanes had been determined from outcrops near VABM Ruby in the Ambler River quadrangle, one of the authors suggested the possibility of a 1.29 b.y. isochron, shown by the short line on Figure 4, but pointed out that these preliminary data were insufficient to rule out the possibility of inherited argon (Turner, 1973). The greater amount of data now available indicates that this line is an "errorchron;" a result of the inherited argon problem combined with insufficient data early in the study.

2. Two glaucophanes from Ruby Ridge, as well as five other minerals (1 muscovite, 1 hornblende, 2 actinolites and 1 glaucophane) from the western extension of the schist belt in the eastern Baird Mountains quadrangle, do plot in a colinear array. This is suggestive evidence, but not proof, that these particular samples may have incorporated inherited  $^{40}\text{Ar}$  of the same isotopic composition during metamorphic recrystallization. Indeed, the fact that any group of minerals form a colinear array on such a diagram does not prove they satisfy this assumption, but merely is consistent with the assumption. The y-intercept of this isochron is zero, suggesting, according to the systematics of the isochron model, that significant amounts of inherited argon are not present in the minerals which plot on the isochron. These minerals are listed on Table 1.
3. In Figure 3, the isochron may appear to be completely dominated by the leverage of the muscovite point. However, if this point is eliminated, the recalculated isochron age is 695 m.y. Moreover, if both the muscovite and hornblende points are

eliminated, as well as the five glaucophanes near the origin which clearly contain significant amounts of inherited  $^{40}\text{Ar}$ , the remaining 5-point amphibole array gives an isochron age of 633 m.y. in excellent agreement with the 12 mineral 634 m.y. isochron; and with a correlation coefficient of 0.975. These relationships may be seen graphically in Figure 4. Although these observations do not prove the validity of the assumption discussed above, they do support the basic K-Ar individual age evidence for a late Precambrian metamorphism in the schist belt, and we believe that the muscovite age of  $636 \pm 38$  m.y. represents a minimum age for the metamorphism.

The concentration of anomalously old glaucophane ages in the metabasites of Ruby Ridge vs the 622-756 m.y. glaucophane, actinolite, hornblende, and muscovite ages from the western segment of the belt, has caused some workers to suggest that the two segments of the belt may be separated by a regional unconformity or suture zone, and that the two schist terranes are of different crystallization ages. This interpretation is supported by the occurrence of a Paleozoic fauna in a dolomitic marble outcropping within the schist belt in the southwestern Survey Pass quadrangle, as discussed in a following section.

We do not favor this interpretation because the lithologies of both areas are very similar, and the unique coarse-grained fabrics displayed in the blueschists derived from gabbros and diabasic rocks on Ruby Ridge, are also present in the western part of the belt which produced the 622-756 m.y. mineral ages. These blueschists contain some of the largest glaucophane grains ever reported from world-wide blueschist belts, and the fabrics of the metabasites derived from mafic igneous

rocks in both areas are remarkable similar, including the record of subsequent retrograde greenschist facies metamorphism.

If the two areas are indeed segments of the same metamorphic belt, why then are the anomalous glaucophane ages confined to Ruby Ridge?

There are several possible explanations, including the following:

- (1) The inherited argon in the low-potassium sodic amphiboles from Ruby Ridge may be due to high argon partial pressures related to P/T conditions of the high pressure sub facies of blueschist metamorphism. This premise is supported by two jadeite occurrences: relict coarse-grained jadeite in a metawacke from Ruby Ridge and jadeite megacrysts in a metabasite from the ridge between the Kogoluktuk and Maneluk Rivers -- the only occurrences reported from the Brooks Range schist belt.
- (2) If the 622-756 m.y. metamorphic cooling ages are valid, then the age of the parental sediments and igneous rocks may be much older. The section could include mafic igneous rocks of varying ages including much older Precambrian basalt flows, as well as somewhat younger mafic sills and dikes. Prior to metamorphism, the older mafic igneous rocks would have accumulated the most radiogenic argon, possibly causing high argon partial pressures during low temperature-high pressure metamorphism. This would amplify the inherited argon problem, and could cause the erroneously old ages.

## REGIONAL RADIOMETRIC EVIDENCE FOR THE AGE OF THE SCHIST BELT

In addition to the K-Ar data, there is a considerable body of regional radiometric evidence which is compatible with the existence of a late Precambrian metamorphic basement in the southwest Brooks Range:

1. To the north, in wells that penetrate greenschist facies basement at Prudhoe Bay, cores have yielded similar late Precambrian to early Cambrian K-Ar ages (Drumond, 1974; I. Tailleux, personal communication). A reasonable structural interpretation of these ages and our Brooks Range data is that the entire Brooks Range is underlain by late Precambrian basement.

2. To the southwest, paragneisses in the Kigluaik Mountains of the Seward Peninsula have been dated as late as Precambrian by Carl Hedge (personal communication) using the Rb-Sr whole-rock isochron technique. The Seward Peninsula Precambrian basement terrane is apparently on trend with the southern bend of the schist belt in the Baird Mountains quadrangle (Beikham and Lathram, 1976).

3. To the east, in the Doonarek structural high of the Central Brooks Range, Dutro, et al. (1976) obtained conventional K-Ar ages and an  $^{40}\text{Ar}/^{39}\text{Ar}$  age plateau of 470 m.y. (early Ordovician) for mafic dikes intruding greenschist facies basement, indicating that the basement is at least as old as early Ordovician in this area.

## PALEONTOLOGIC EVIDENCE FOR THE AGE OF THE SCHIST BELT

Paleontologic evidence from a fossil locality in the southwestern Survey Pass quadrangle is in apparent conflict with the body of radiometric evidence discussed above. A dolomitic marble lens apparently within the schist belt has recently produced fairly well preserved corals, bryozoans and crinoid columnals indicating a Paleozoic age (Brosgé and Pessel, 1977, fossil locality 17; I. L. Tailleux, personal communication).

One possible explanation for this apparent age conflict is that the marble lens may be tectonically infolded or imbricated within the schist belt. Such a structural situation is certainly possible in a metamorphic terrane characterized by overturned, subisoclinal folds and thrusts (Forbes and others, 1973).

## EVIDENCE OF REGIONAL METAMORPHISM FROM THE STRATIGRAPHIC RECORD

### The Late Mesozoic Metamorphism

There are two lines of evidence from the stratigraphic record which reveal the history of the late Mesozoic metamorphism in the southern Brooks Range. First, by reconstructing the history of the Late Mesozoic orogeny which must have accompanied the metamorphism, the probable timing of the metamorphic event can be outlined. Secondly, Cretaceous bentonites flanking the Brooks Range are believed to represent extrusive equivalents of the late synkinematic granite intrusives in the schist belt, and thus may be used to date the end of schist belt metamorphism.

The stratigraphic record from northern Alaska indicates that the ancestral Brooks Range began to form in the Late Jurassic. The best record of this comes from the North Slope where great volumes of immature flysch-like sediments were deposited in the basin adjacent to the uplift from late Jurassic to mid-Cretaceous time. This sedimentation reflected the period of major tectonism which was characterized by large-scale flat thrust sheets composed of unmetamorphosed preorogenic and penecontemporaneous sediments in the northern half of the Brooks Range. The end of immature sedimentation registers the cessation of major thrusting sometime in the Albian Stage about 100 million years ago (Tailleur and Brosge, 1970).

Regional metamorphism probably began as the relatively autochthonous rocks of the southern Brooks Range became depressed and squeezed as great thrust panels were successively imbricated and stacked above them. As major tectonism waned in the Late Cretaceous, it is probable that metamorphism came to an end, and this history is supported by most K-Ar

cooling ages of 86 to 130 m.y. obtained from muscovite and biotite collected in the schist belt. Although it is likely that the Brooks Range has remained a positive area since the end of the Cretaceous, and few localities show moderate deformation of Late Cretaceous sediments, there is no evidence of Cenozoic orogeny that would produce a regional metamorphism in the Western Brooks Range.

Another line of evidence which records the end of metamorphism comes from the granitic plutons cropping out in the center of the metamorphic belt. Although the granitic rocks are themselves predominantly metamorphosed, parts of the interiors of some of the plutons, such as at Arrigetch Peaks, show nonfoliated texture, while the borders are strongly foliated. This may indicate that the interior parts of some plutons solidified after most of the metamorphic stress had been relieved. In addition, thermal aureoles around the granitic bodies have sometimes caused incipient thermal metamorphic minerals to develop with random orientation in host rocks having strong foliation. This evidence suggests that the metamorphic belt was intruded by late stage synkinematic granitic plutons. It also seems likely that there was volcanism associated with this intrusive stage because mid-Cretaceous sediments north and south of the Brooks Range contain rhyolitic tuffs which have micas yielding K-Ar ages of about 83 to 91 m.y. (I. L. Tailleux, personal communication). These dates agree with K-Ar dates from the plutons themselves, as discussed previously.

#### The Question of Pre-Late Mesozoic Metamorphism

Was a metamorphic terrane present in the southern Brooks Range prior to the late Mesozoic metamorphism? The body of evidence from the

stratigraphic record supporting the existence of an old metamorphic terrane is not large; nor is it conclusive for or against such a terrane. It comes from two sources. The first is a study of heavy minerals in sediments derived from the late Mesozoic orogeny. The second comes from a sedimentary rock unit containing metamorphic minerals and rock fragments which may be Paleozoic in age.

During the petroleum exploration program conducted in Naval Petroleum Reserve No. 4 from 1944 to 1953, heavy mineral studies were conducted from selected samples in the various wells which penetrated Jurassic and Cretaceous sediments. A compilation of this data relating the occurrences of heavy minerals to geologic units has been made by R. H. Morris and E. H. Lathram (1951) and more recently by I. L. Tailleux (unpublished data, 1977). Three of the minerals studied (garnet, chloritoid, and glaucophane) have a probable metamorphic origin. Garnet is found as a moderately abundant mineral in Late Jurassic through Cretaceous rocks but is not identified in preorogenic sediments of the Early Jurassic and Triassic. Chloritoid is first found rarely in Late Jurassic and Early Cretaceous sediments from a few wells and is absent in the others. It is not until the mid-Cretaceous that chloritoid becomes a common constituent in the sediments. Glaucophane is not found until it suddenly appears in the mid-Cretaceous, after which it is a common constituent.

The presence of garnet in some of the first sediments to be shed from the orogenic belt in the Late Jurassic suggests the possibility that old metamorphic rocks may have been uplifted and eroded at the onset of orogeny. However, because of the variety of ways in which garnet may occur and the possibility of it being reworked through many erosional cycles or being transported great distances, the occurrence of

garnet by itself must be considered inconclusive. The rare presence of chloritoid in early orogenic sediments does support the possibility of an old metamorphic terrane. The occurrence of glaucophane suggests that if this glaucophane was present in old metamorphic rocks, it was not unroofed by northward flowing streams until mid-Cretaceous time. Alternatively, glaucophane may not have been present in pre-Jurassic metamorphic rocks but may have been formed in the Late Jurassic or Early Cretaceous and then eroded in the mid-Cretaceous.

Unfortunately, heavy mineral studies have not been conducted from Late Jurassic and Early Cretaceous sediments on the south side of the Brooks Range. Since these orogenic sediments are more proximal to the metamorphic belt, such a study could give important clues as to the character of the early orogenic terrane.

The second line of evidence dealing with the possibility of an old metamorphic terrane comes from a feldspathic graywacke occurring along the north edge of the metamorphic rocks in the Ambler River and Baird Mountains quadrangles. Petrologic examination of this unit from the Nanielik Creek area in northwestern Ambler River quadrangle, where metamorphic recrystallization is minimal, has revealed that it contains low grade metamorphic detrital rock fragments. In addition, numerous examples of detrital garnet are found, some of which have helicitic texture revealing a dynamothermal metamorphic origin. The mineralogic and lithologic makeup of this wacke is similar in composition to Cretaceous feldspathic graywacke occurring along the southern margin and in the northern half of the Brooks Range. However, field evidence supports an early Paleozoic age assignment for this unit, because at one locality it is overlain by Mississippian conglomerate and in another it is apparently

interbedded with Devonian carbonate. However, at neither of these localities can it be stated with certainty that shearing and faulting are not responsible for the observed relationships. If, in the future, the age of this wacke can be shown conclusively to be Early Paleozoic, there will be conclusive stratigraphic evidence of an old metamorphic terrane in the southern Brooks Range.

It is apparent from the previous discussion that stratigraphic evidence for or against the existence of a pre-Late Mesozoic metamorphic terrane is inconclusive. However, the occurrence of metamorphic minerals in Mesozoic and Paleozoic(?) sediments leaves open the possibility that there may have been an old metamorphic terrane in the southern Brooks Range which has been subsequently remetamorphosed in the Late Mesozoic.

## SUMMARY AND CONCLUSIONS

The southwestern Brooks Range schist belt has had a complex geologic history, as reflected in part by the complex pattern of radiometric ages discussed above. The presently-available radiometric age evidence suggests that this schist belt has, at least in part, undergone a late Precambrian metamorphism, and that the parent sedimentary and igneous rocks for the dated Precambrian metamorphics are at least as old as Late Precambrian (Precambrian Z). We speculate that the Paleozoic marble in the Survey Pass quadrangle is either:

1. infolded or tectonically imbricated in the schist belt, or
2. there is a presently unrecognized structural or stratigraphic discontinuity of some kind between this marble and schists radiometrically dated as Late Precambrian.

The schist terrane experienced a major thermal event in mid-Cretaceous time, causing widespread resetting of nearly all K-Ar mica ages. This thermal event may have been synchronous with the emplacement of the E-W-trending series of granitic plutons discussed above.

Two areas studied in this schist terrane, in the eastern Baird Mountains and Ambler River quadrangles, have apparently preserved K-Ar age evidence of a previous, Late Precambrian metamorphism. As seen in Figure 2, there are a number of apparent ages intermediate between Late Precambrian and Cretaceous. These intermediate ages are interpreted as indicating varying amounts of partial argon loss from older rocks during the Cretaceous event. Further work will be aimed at testing this hypothesis using the  $^{40}\text{Ar}/^{39}\text{Ar}$  incremental heating technique.

#### ACKNOWLEDGEMENTS

We wish to thank Irv Tailleux, Gil Mull and John Carden for many lively and stimulating discussions of Brooks Range geology. We are grateful to Gar Pessel, Bill Brosge and Irv Tailleux for making their previously unpublished geologic mapping available for use in Plate 1. Diane Duvall provided laboratory assistance with mineral separations, K-Ar measurements, and mass spectrometry. The manuscript was reviewed by Bill Brosge and Marvin Lanphere.

## REFERENCES

- Beikman, H. M. and E. H. Lathram, 1976, Preliminary geologic map of northern Alaska, U.S. Geol. Survey Map MF 789.
- Brosge, W. P. and H. N. Reiser, 1971, Preliminary geologic map, Wiseman and eastern Survey Pass quadrangles, Alaska, U.S. Geol. Survey Open File Map 479, 2 sheets, scale 1:250,000.
- Brosge, W. P. and G. H. Pessel, 1977, Preliminary reconnaissance geologic map of Survey Pass quadrangle, Alaska. U.S. Geol. Survey Open File Map OF 77-27.
- Drummond, K. J., 1974, Paleozoic arctic margins of North America in Burke, C.A., and Drake, C. L. The geology of continental margins, Springer-Verlag, NY, 1009 p., p. 802.
- Dutro, J. T., W. P. Brosge, M. A. Lanphere, and H. N. Reiser, 1976, Geologic significance of Doonerak structural high, central Brooks Range, Alaska, AAPG Bull, V. 60 No. 6, pp 952-961.
- Forbes, R. B., D. L. Turner. W. G. Gilbert and J. R. Carden, 1974, Ruby Ridge Traverse, southwestern Brooks Range, in Hartman, D., ed., Alaska, Div. Geol. and Geophys. Surveys 1973 Ann. Rept., pp 34-35.
- Fritts, C. E., Eakins, G. R., and R. E. Garland, 1972, Geology and geochemistry near Walker Lake, southern Survey Pass quadrangle, arctic Alaska: Alaska Div. Geol. Survey 1971 Ann. Rept., p. 19-26.
- Morris, R. H. and E. H. Lathram, 1951, Heavy mineral studies in the geology of the arctic slope of Alaska, by Payne and others, Oil and Gas Investigations, Map OM 126 (sheet 3).
- Patton, W. W., Jr., and T. P. Miller, 1968, Regional geologic map of the Selawik and southeastern Baird Mountains quadrangles, Alaska, U.S. Geol. Survey Misc. Geol. Inv. Map I-530, 1 sheet, scale 1:250,000.
- Pessel, G. H., Garland, R. E., Tailleux, I. L. and G. R. Eakins, 1973, Preliminary geologic map of southeastern Ambler River and part of Survey Pass quadrangle, Alaska: Alaska Div. Geol. and Geophys. Surveys Open-File Rept. 36.
- Tailleux, I. L. and W. P. Brosge, 1970, Tectonic history of northern Alaska; Proceedings of the Geological Seminar on the North Slope of Alaska, Pacific Section Amer. Assoc. of Petroleum Geologists, p. E1-E20.
- Taylor, H. P., and R. G. Coleman, 1968,  $^{18}\text{O}/^{16}\text{O}$  ratios of co-existing minerals in glaucophane-bearing metamorphic rocks: Geol. Soc. America Bull., v. 79, p. 1727-1756.

Turner, D. L., R. B. Forbes and C. W. Naeser, 1975, Radiometric ages of Kodiak Seamount and Giacomini Guyot, Gulf of Alaska: implications for circum-Pacific tectonics, *Science*, V. 182, pp 579-581.

Turner, D. L., 1974, Geochronology in Alaska-1973, in Hartman, D., ed., State of Alaska Dept. of Natural Resources, Division of Geological and Geophysical Surveys, 1973 Ann. Rept., pp 25-30.

Table 2. Analytical Data for K-Ar Determinations

| Sample No.<br>(Lab No.) Quad.          | Rock Type | Mineral<br>Dated | K <sub>2</sub> O<br>(weight<br>percent)  | Sample<br>Weight<br>(grams) | $\frac{40}{\text{Ar}}_{\text{rad}}$<br>(moles/gm)<br>$\times 10^{-11}$ | $\frac{40}{\text{Ar}}_{\text{rad}}$<br>$\frac{40}{\text{K}}$<br>$\times 10^{-3}$ | $\frac{40}{\text{Ar}}_{\text{rad}}$<br>$\frac{40}{\text{Ar}}$<br>total | Apparent K-Ar Age<br>$\pm 1 \sigma$ (m.y.) |
|--|-----------|------------------|--|-----------------------------|--|--|--|--|
| 55-ATR 109<br>(76161) AR               | TremSch   | tremolite        | 0.030<br>0.025<br>0.026<br>0.032<br>0.030<br>0.032<br>0.032<br>0.029<br>0.030<br>$\bar{x} = 0.030$ | 1.3898                      | 1.456  | 19.55  | 0.503  | 308 $\pm$ 30.8                             |
| 71 F 17<br>(72083) SP                  | BioHusGns | biotite          | 9.415<br>9.392<br>$\bar{x} = 9.403$  | 0.7318                      | 128.1  | 5.392  | 0.847  | 90.0 $\pm$ 2.7                             |
| 72 E 568<br>(73057) AR                 | BioHusSch | muscovite        | 10.990<br>11.010<br>$\bar{x} = 11.000$   | 0.1648                      | 307.2  | 11.06  | 0.881  | 180 $\pm$ 5.4                              |
| 72 E 100R<br>(73056) AR                | QtzHusSch | muscovite        | 10.240<br>10.250<br>$\bar{x} = 10.245$   | 0.1562                      | 197.4  | 7.628  | 0.931  | 126 $\pm$ 3.8                              |
| 72 E 222<br>(73058) AR                 | GrGns     | biotite          | 8.620<br>8.580<br>$\bar{x} = 8.605$  | 0.3352                      | 122.1  | 5.617  | 0.927  | 93.6 $\pm$ 2.8                             |
| 72 E 222<br>(73055) AR                 | GrGns     | muscovite        | 10.940<br>10.970<br>$\bar{x} = 10.955$   | 0.2134                      | 162.6  | 5.878  | 0.950  | 97.9 $\pm$ 2.9                             |
| 72 F 10ARG2<br>(72159) SP              | Grnsch    | actinolite       | 0.029<br>0.030<br>0.029<br>0.028<br>0.031<br>0.042<br>0.036<br>0.031<br>0.032<br>$\bar{x} = 0.032$ | 1.0159                      | 1.461  | 18.14  | 0.149  | 287 $\pm$ 57.4                             |
| 72 F 10ARG2<br>(72161) SP<br>Replicate | Grnsch    | actinolite       | "  | 0.9988                      | 1.477  | 18.28  | 0.174  | 289 $\pm$ 57.8<br>$\bar{x} = 288 \pm 57.6$ |
| 72 C 211<br>(73011) SP                 | BioQtzSch | biotite          | 9.197<br>9.169<br>$\bar{x} = 9.183$  | 0.2073                      | 134.2  | 5.785  | 0.814  | 96.4 $\pm$ 2.9                             |
| 72 Pe 92<br>(74002) AR                 | BioHusGns | biotite          | 8.440<br>8.430<br>$\bar{x} = 8.435$  | 0.3477                      | 111.4  | 5.230  | 0.852  | 87.3 $\pm$ 2.6                             |

| Sample No.<br>(Lab No.) Quad.          | Rock Type      | Mineral Dated    | K <sub>2</sub> O<br>(weight percent)                  | Sample Weight (grams) | $\frac{40}{Ar} \text{ rad}$<br>(moles/gm)<br>$\times 10^{-11}$ | $\frac{40}{Ar} \text{ rad}$<br>$\frac{40}{K} \times 10^{-3}$ | $\frac{40}{Ar} \text{ rad}$<br>$\frac{40}{Ar} \text{ total}$ | Age $\pm 1 \sigma$<br>(m.y.) |
|--|----------------|------------------|---|-----------------------|--|--|--|------------------------------|
| 72 Pe 92<br>(73060) AR<br>Replicate    | GioMusGns      | biotite          | "   | 0.2922                | 109.5  | 5.139  | 0.807  | 85.8 $\pm$ 2.6               |
|  |                |                  |   |                       |  |  |  | $\bar{x} = 86.5 \pm 2.6$     |
| 72 Pe 92<br>(73059) AR                 | BioMusGns      | muscovite        | 10.980<br>10.970<br>11.000<br>$\bar{x} = 10.983$      | 0.2170                | 189.1  | 6.815  | 0.958  | 113 $\pm$ 3.4                |
| 73 ABe 108<br>(75073) SP               |                | biotite          | 6.297<br>6.292<br>6.294<br>$\bar{x} = 6.294$          | 0.2545                | 93.38  | 5.873  | 0.694  | 97.8 $\pm$ 2.9               |
| 73 ABe 108<br>(74171) SP               |                | hornblende       | 0.176<br>0.180<br>0.178<br>$\bar{x} = 0.178$          | 1.1292                | 3.063  | 6.813  | 0.509  | 113 $\pm$ 3.4                |
| 73 ATr 15.2<br>(74182) SP              | BioMusFeld-Sch | biotite          | 8.755<br>8.810<br>8.782<br>$\bar{x} = 8.782$          | 0.3056                | 136.5  | 6.153  | 0.900  | 102 $\pm$ 3.1                |
| 73 ATr 15.2<br>(75051) SP              | BioMusFeld-Sch | muscovite        | 10.457<br>10.442<br>10.449<br>$\bar{x} = 10.449$      | 0.3750                | 183.6  | 6.955  | 0.897  | 115 $\pm$ 3.5                |
| 73 ATr 20.2<br>(74084) SP              | QtzMusSch      | muscovite        | 10.138<br>10.162<br>10.150<br>$\bar{x} = 10.150$      | 0.5408                | 174.0  | 6.786  | 0.950  | 113 $\pm$ 3.4                |
| 73 ATr 45.2<br>(74179) SP              | Grnsch         | actinolite       | 0.140<br>0.130<br>0.130<br>0.130<br>$\bar{x} = 0.132$ | 2.1078                | 3.411  | 10.19  | 0.595  | 167 $\pm$ 8.3                |
| 73 ATr 45.2<br>(74179) SP<br>Replicate | Grnsch         | actinolite       | "   | 2.1078                | 3.482  | 10.40  | 0.602  | 170 $\pm$ 8.5                |
|  |                |                  |   |                       |  |  |  | $\bar{x} = 168 \pm 8.4$      |
| 73 ATr 45.2<br>(75068) SP              | Grnsch         | impure muscovite | 9.257<br>9.357<br>9.307<br>$\bar{x} = 9.307$          | 0.1790                | 162.0  | 6.889  | 0.906  | 114 $\pm$ 3.4<br>Minimum Age |
| 73 ATr 105.4<br>(74091) AR             | BioMusFeld-Sch | biotite          | 8.228<br>8.228<br>8.228<br>$\bar{x} = 8.228$          | 0.2374                | 127.8  | 6.150  | 0.749  | 102 $\pm$ 3.1                |
| 73 ATr 105.4<br>(75079) AR             | BioMusFeld-Sch | muscovite        | 11.163<br>11.107<br>11.135<br>$\bar{x} = 11.135$      | 0.2936                | 190.3  | 6.766  | 0.849  | 112 $\pm$ 3.4                |

| Sample No.<br>(Lab No.) Quad.        | Rock Type             | Mineral Dated          | K <sub>2</sub> O<br>(weight percent)                                    | Sample Weight (grams) | $\frac{40}{K} \frac{Ar_{rad}}{Ar}$ x 10 <sup>-3</sup> | $\frac{40}{Ar} \frac{Ar_{rad}}{total}$ | Age ± 1 σ (m.y.)                     |
|--------------------------------------|-----------------------|------------------------|---|-----------------------|---|--|--------------------------------------|
| 73 B 33<br>(74085) SP                | MuscFeldSch           | muscovite              | $\bar{x} = 11.30$<br>11.31<br>11.31                                     | 0.3099                | 6.61  | 0.881                                  | 110 ± 3.3                            |
| 73 G 64<br>(74170) SP                | CalcTremSch           | tremolite              | 0.137<br>0.127<br>0.127<br>$\bar{x} = 0.129$                            | 1.8489                | 12.38   | 0.529                                  | 200 ± 12.0                           |
| 73 Re 58<br>(74137) SP               | MuscFeldSch           | muscovite              | 8.713<br>8.685<br>$\bar{x} = 8.699$                                     | 0.5203                | 6.404   | 0.892                                  | 106 ± 3.2                            |
| 73 Pe 32<br>(74086) SP               | CalcHusSch            | muscovite              | 10.212<br>10.200<br>$\bar{x} = 10.206$                                  | 0.3467                | 8.257   | 0.905                                  | 136 ± 4.1                            |
| 73 RR 6EF<br>(75129) AR              | BioFeldQtz-<br>HusSch | biotite                | 9.530<br>9.530<br>$\bar{x} = 9.530$                                     | 0.4304                | 6.115   | 0.888                                  | 102 ± 3.0                            |
| 73 RR 6EF<br>(75126) AR<br>Replicate | BioFeldQtz-<br>HusSch | biotite                | "   | 0.3416                | 6.199   | 0.934                                  | 103 ± 3.0<br>$\bar{x} = 102 \pm 3.0$ |
| 73 RR 6EF<br>(75039) AR              | BioFeldQtz-<br>HusSch | muscovite              | 11.222<br>11.172<br>$\bar{x} = 11.197$                                  | 0.4417                | 6.725   | 0.928                                  | 112 ± 3.3                            |
| 73 RR 7G<br>(75001) AR               | GlcQtzHusSch          | glaucoaphane           | 0.038<br>0.038<br>$\bar{x} = 0.038$                                     | 2.2151                | 40.29   | 0.525                                  | 587 ± 58                             |
| 73 RR 7G<br>(75002) AR               | GlcQtzHusSch          | muscovite              | 5.092<br>5.030<br>$\bar{x} = 5.061$                                     | 0.2631                | 7.534   | 0.651                                  | 125 ± 3.7                            |
| 73 RR 10-1C<br>(75083) AR            | QtzHusSch             | muscovite              | 9.692<br>9.698<br>$\bar{x} = 9.695$                                     | 0.1930                | 7.768   | 0.875                                  | 128 ± 3.8                            |
| 73 RR 18F<br>(74183) AR              | BioQtzHusSch          | biotite                | 9.140<br>9.097<br>$\bar{x} = 9.118$                                     | 0.2140                | 7.815   | 0.910                                  | 129 ± 3.9                            |
| 73 RR 18F<br>(75052) AR              | BioQtzHusSch          | muscovite              | 10.796<br>10.878<br>$\bar{x} = 10.837$                                  | 0.2766                | 7.688   | 0.849                                  | 127 ± 3.8                            |
| 73 RR 31C<br>(75028) AR              | GlcSch                | impure<br>glaucoaphane | 0.027<br>0.031<br>0.030<br>0.028<br>0.023<br>0.028<br>$\bar{x} = 0.028$ | 1.2121                | 38.14   | 0.568                                  | 560 ± 67<br>Minimum Age              |

Sample No.  
(Lab. No.) Quad.

Rock Type

Mineral Dated

K<sub>2</sub>O (weight percent)

Sample Weight (grams)

$\frac{40_{Ar}}{40_{K}} \times 10^{-3}$

$\frac{40_{Ar}}{40_{Ar}} \text{ total}$

Apparent K-Ar Age  $\pm 1 \sigma$  (m.y.)

| Sample No.<br>(Lab. No.) Quad.      | Rock Type | Mineral Dated     | K <sub>2</sub> O (weight percent)  | Sample Weight (grams) | $\frac{40_{Ar}}{40_{K}} \times 10^{-3}$ | $\frac{40_{Ar}}{40_{Ar}} \text{ total}$ | Apparent K-Ar Age $\pm 1 \sigma$ (m.y.)        |
|-------------------------------------|-----------|-------------------|--|-----------------------|---|---|--|
| 73 RR 45C<br>(76077) AR             | ActSch    | actinolite        | 0.110<br>0.109<br>0.115<br>0.109<br>0.114<br>0.112<br>0.113<br>$\bar{x} = \frac{0.106}{0.111}$ | 0.6016                | 9.707                                   | 0.418                                   | 159 $\pm$ 6.4                                  |
| 73 RR 52<br>(75025) AR              | GarGlcSch | glaucophane       | 0.035<br>0.036<br>0.034<br>$\bar{x} = \frac{0.035}{0.035}$                                     | 2.4121                | 42.21                                   | 0.669                                   | 611 $\pm$ 30.5                                 |
| 73 RR 52<br>(75019) AR<br>Replicate | GarGlcSch | glaucophane       | "  | 2.7135                | 45.33                                   | 0.687                                   | 649 $\pm$ 32.5<br>$\bar{x} = 630 \pm 31.5$     |
| 73 RR 54<br>(75023) AR              | GarGlcSch | glaucophane       | 0.038<br>0.037<br>0.037<br>$\bar{x} = \frac{0.037}{0.037}$                                     | 1.2438                | 160.3                                   | 0.817                                   | * 1690 $\pm$ 84.5                              |
| 73 RR 54<br>(75020) AR<br>Replicate | GarGlcSch | glaucophane       | "  | 2.0064                | 159.0                                   | 0.826                                   | * 1680 $\pm$ 84.0<br>$\bar{x} = 1685 \pm 84.2$ |
| 73 RR 75-3<br>(76197) AR            | ActSch    | impure actinolite | 0.075<br>0.072<br>0.069<br>$\bar{x} = \frac{0.068}{0.071}$                                     | 1.3220                | 0.221                                   | 0.641                                   | 345 $\pm$ 17.3<br>Minimum Age                  |
| 74 ABe 21B<br>(75097) BN            | GrnSch    | actinolite        | 0.045<br>0.044<br>0.044<br>0.045<br>0.044<br>$\bar{x} = \frac{0.045}{0.044}$                   | 0.7047                | 19.97                                   | 0.156                                   | 314 $\pm$ 15.7                                 |
| 74 ABe 222F<br>(75091) BN           | GarGlcSch | phlogopite        | 9.810<br>9.816<br>$\bar{x} = \frac{9.813}{9.813}$  | 0.4447                | 5.865                                   | 0.868                                   | 97.7 $\pm$ 2.9                                 |
| 74 AF 144-3<br>(74125) BN           | AmpSch    | actinolite        | 0.090<br>0.091<br>0.095<br>0.088<br>$\bar{x} = \frac{0.091}{0.091}$                            | 0.7952                | 43.14                                   | 0.646                                   | 622 $\pm$ 31.1                                 |
| 74 AF 145-1<br>(74122) BN           | MusSch    | muscovite         | 9.192<br>9.512<br>$\bar{x} = \frac{9.352}{9.352}$  | 0.2693                | 44.43                                   | 0.978                                   | 638 $\pm$ 38.3                                 |

| Sample No.<br>(Lab No.) Quad.           | Rock Type     | Mineral<br>Dated | K <sub>2</sub> O<br>Weight<br>percent                          | Sample<br>Weight<br>(Grams) | $\frac{^{40}\text{Ar rad}}{^{40}\text{K}} \times 10^{-11}$ | $\frac{^{40}\text{Ar rad}}{^{40}\text{K}} \times 10^{-3}$ | $\frac{^{40}\text{Ar rad}}{^{40}\text{Ar total}}$ | Apparent K-Ar Age<br>$\pm 1 \sigma$ (m.y.) |
|---|---------------|------------------|--|-----------------------------|--|---|---|--|
| 74 AF 145-5<br>(74124) BM               | AmphSch       | hornblende       | 0.740<br>0.740<br>0.740<br>$\bar{x} = 0.740$                   | 1.1514                      | 95.76  | 51.23   | 0.956   | 719 $\pm$ 21.6                             |
| 74 AF 155-13<br>(75017) BM              | QtzParGlcSch  | glaucophane      | 0.052<br>0.051<br>0.052<br>0.053<br>$\bar{x} = 0.052$          | 2.1509                      | 7.119  | 54.20   | 0.793   | 753 $\pm$ 45.2                             |
| 74 AF 155-13<br>(74121) BM<br>Replicate | QtzParGlcSch  | glaucophane      | "  | 1.5090                      | 7.175  | 54.63   | 0.688   | 758 $\pm$ 45.5                             |
| 74 AF 155-13<br>(75044) BM              | QtzParGlcSch  | paragonite       | 0.373<br>0.373<br>0.373<br>$\bar{x} = 0.373$                   | 0.2060                      | 11.37  | 12.07   | 0.357   | $\bar{x} = 756 \pm 45.4$<br>196 $\pm$ 5.9  |
| 74 AF 155-13<br>(74129) BM<br>Replicate | QtzParGlcSch  | paragonite       | "  | 0.2921                      | 10.80  | 11.46   | 0.187   | 186 $\pm$ 5.6                              |
| 74 ATR 129-7<br>(75082) BM              | GrnSch        | actinolite       | 0.088<br>0.088<br>0.086<br>0.089<br>0.088<br>$\bar{x} = 0.088$ | 0.3723                      | 10.09  | 45.52   | 0.610   | 651 $\pm$ 39.1                             |
| 74 ATR 150-3<br>(75117) BM              | BlotusFeldSch | blotite          | 8.898<br>8.882<br>8.890<br>$\bar{x} = 8.890$                   | 0.5191                      | 149.9  | 6.674   | 0.939   | 111 $\pm$ 3.3                              |
| 74 ATR 150-3<br>(75119) BM              | BlotusFeldSch | muscovite        | 10.420<br>10.450<br>10.435<br>$\bar{x} = 10.435$               | 0.1513                      | 176.2  | 6.685   | 0.788   | 111 $\pm$ 3.3                              |
| 74 AM 309<br>(75058) AR                 | ActQtzChlSch  | actinolite       | 0.076<br>0.076<br>0.079<br>0.070<br>0.075<br>$\bar{x} = 0.075$ | 1.1769                      | 5.335  | 28.07   | 0.499   | 427 $\pm$ 29.9                             |
| 74 AM 1535-3<br>(75077) AR              | FeldSch       | blotite          | 8.668<br>8.633<br>8.650<br>$\bar{x} = 8.650$                   | 0.1221                      | 149.4  | 6.838   | 0.915   | 113 $\pm$ 3.5                              |
| 74 AM 1535-3<br>(75046) AR              | FeldSch       | muscovite        | 10.528<br>10.550<br>10.539<br>$\bar{x} = 10.539$               | 0.3418                      | 188.3  | 7.074   | 0.943   | 117 $\pm$ 3.5                              |
| 74 AF 145-1<br>(75045) BM<br>Replicate  | MusSch        | muscovite        | "  | 0.1171                      | 1042   | 44.12   | 0.969   | 634 $\pm$ 25.4<br>$\bar{x} = 636 \pm 38.2$ |

| Sample No.<br>(Lab No.) Quad.  | Rock Type          | Mineral<br>Dated | K <sub>2</sub> O<br>(Weight<br>percent)   | Sample<br>Weight<br>(grams) | $\frac{40 \text{ Ar rad}}{40 \text{ K}} \times 10^{-3}$ | $\frac{40 \text{ Ar rad}}{40 \text{ Ar total}}$ | Apparent K-Ar Age<br>$\pm 1 \sigma$ (m.y.)   |
|--------------------------------|--------------------|------------------|---|-----------------------------|---|---|--|
| 74 Pe 2B<br>(75115) BM         | BioMusGns          | biotite          | 9.402<br>9.350<br>$\bar{x} = 9.376$   | 0.3851                      | 5.614   | 0.903   | 93.6 $\pm$ 2.8                               |
| 74 Pe 2B<br>(75124) BM         | BioMusGns          | muscovite        | 11.017<br>11.012<br>$\bar{x} = 11.014$  | 0.5252                      | 6.263   | 0.953   | 104 $\pm$ 3.1                                |
| 74 Pe 121<br>(75090) BM        | QtzMusSch          | muscovite        | 7.598<br>7.520<br>$\bar{x} = 7.559$   | 0.4322                      | 7.140   | 0.867   | 118 $\pm$ 3.5                                |
| 75 AM 3<br>(76028) AR          | BioMusFeld-<br>Gns | biotite          | 9.325<br>9.332<br>$\bar{x} = 9.328$   | 0.3673                      | 6.036   | 0.941   | 100 $\pm$ 3.0                                |
| 75 AM 3<br>(76028) AR          | BioMusFeld<br>Gns  | muscovite        | 10.322<br>10.390<br>10.542<br>10.630<br>$\bar{x} = 10.471$                                | 0.1849                      | 6.932   | 0.924   | 115 $\pm$ 3.4                                |
| 75 AM 1500<br>(76010) AR       | FeldSch            | muscovite        | 10.753<br>10.893<br>10.700<br>10.875<br>$\bar{x} = 10.805$                                | 0.2942                      | 9.746   | 0.892   | 160 $\pm$ 4.8                                |
| 74 AM 1745.5<br>(75048) AR     | ActSkarn           | actinolite       | 0.280<br>0.280<br>0.259<br>0.251<br>0.250<br>0.260<br>0.252<br>0.261<br>$\bar{x} = 0.262$ | 2.5572                      | 15.06   | 0.812   | 241 $\pm$ 14.5                               |
| A-1<br>(72156) AR              | GargGlcSch         | glaucophane      | 0.012<br>0.012<br>0.011<br>0.012<br>0.013<br>0.012<br>$\bar{x} = 0.012$                   | 0.7061                      | 316.1   | 0.454   | * 2550 $\pm$ 510                             |
| A-1<br>(72093) AR<br>Replicate | GargGlcSch         | glaucophane      | "   | 0.8324                      | 321.1   | 0.672   | * 2570 $\pm$ 514                             |
| A-1 AR<br>(72156)<br>Replicate | GargGlcSch         | glaucophane      | "   | 0.7865                      | 315.7   | 0.632   | * 2550 $\pm$ 510<br>$\bar{x} = 2557 \pm 511$ |

| Sample No.<br>(Lab No.) Quad. | Rock Type    | Mineral Dated | K <sub>2</sub> O<br>(weight percent)  | Sample Weight (grams) | $\frac{^{40}\text{Ar}_{\text{rad}}}{^{40}\text{Ar}}$<br>(moles/gm) $\times 10^{-11}$ | $\frac{^{40}\text{Ar}_{\text{rad}}}{^{40}\text{K}} \times 10^{-3}$ | $\frac{^{40}\text{Ar}_{\text{rad}}}{^{40}\text{Ar}_{\text{total}}}$ | Apparent K-Ar Age $\pm 1 \sigma$ (m.y.) |
|-------------------------------|--------------|---------------|---|-----------------------|--|--|---|---|
| A-1 CNM<br>(72146) AR         | GarGlcSch    | paragonite    | 0.430<br>$\bar{x} = 0.430$  | 0.5117                | 15.86  | 14.60  | 0.322   | 234 $\pm$ 7                             |
| A-2<br>(72127) AR             | GarGlcSch    | glaucophane   | 0.028<br>0.027<br>0.028<br>0.029<br>$\bar{x} = 0.028$                                     | 3.1826                | 7.501  | 106.1  | 0.839   | * 1270 $\pm$ 254                        |
| A-2<br>(72162) AR             | GarGlcSch    | paragonite    | 0.550<br>0.550<br>$\bar{x} = 0.550$   | 1.9661                | 18.37  | 13.22  | 0.481   | 213 $\pm$ 6                             |
| A-3<br>(72129) AR             | JadGarGlcSch | glaucophane   | 0.015<br>0.015<br>0.015<br>0.015<br>$\bar{x} = 0.015$                                     | 3.1772                | 4.741  | 125.1  | 0.767   | * 1430 $\pm$ 357                        |
| 75 ANM 1501.1<br>(76005) AR   | FeldSch      | muscovite     | 10.625<br>10.890<br>$\bar{x} = 10.758$  | 0.2616                | 191.7  | 7.053  | 0.875   | 117 $\pm$ 3.5                           |
| 75 ANM 1502<br>(75141) AR     | ActSch       | actinolite    | 0.077<br>0.083<br>0.077<br>0.077<br>0.076<br>0.076<br>0.076<br>0.078<br>$\bar{x} = 0.077$ | 0.9585                | 4.932  | 25.19  | 0.380   | 388 $\pm$ 15.5                          |
| 75 ANM 1503.1<br>(76002) AR   | QtzKueSch    | muscovite     | 10.015<br>9.962<br>9.912<br>9.897<br>$\bar{x} = 9.946$                                    | 0.2609                | 160.4  | 6.384  | 0.889   | 106. $\pm$ 3.2                          |
| A-3<br>(72163) AR             | JadGarGlcSch | paragonite    | 0.641<br>0.640<br>0.640<br>$\bar{x} = 0.640$  | 0.7656                | 21.75  | 13.44  | 0.782   | 217 $\pm$ 6.5                           |
| C-2<br>(72125) AR             | GarGlcSch    | glaucophane   | 0.043<br>0.044<br>0.044<br>0.045<br>$\bar{x} = 0.044$                                     | 2.8506                | 12.60  | 113.4  | 0.869   | * 1330 $\pm$ 133                        |

Note: Ages preceded by \* have been increased significantly by inherited argon and do not represent valid cooling ages.

Constants Used:  $\lambda_e = 0.585 \times 10^{-10} \text{ yr}^{-1}$ ,  $\lambda_\beta = 4.72 \times 10^{-10} \text{ yr}^{-1}$ ,  $^{40}\text{K}/\text{K}_{\text{total}} = 1.19 \times 10^{-4} \text{ mol/mol}$ .

Table 3. K-Ar Dates Previously Published by the USGS

| Sample No.<br>(Lab No.) Quad. | Rock Type               | Mineral<br>Dated | K <sub>2</sub> O<br>(weight<br>percent) | Sample<br>Weight<br>(grams) | $^{40}\text{Ar}/\text{rad}$<br>(moles/gm)<br>$\times 10^{-11}$ | $^{40}\text{Ar}/\text{rad}$<br>$^{40}\text{K}$<br>$\times 10^{-3}$ | $^{40}\text{Ar}/\text{rad}$<br>$^{40}\text{Ar}$<br>total | Age $\pm 1 \sigma$<br>(m.y.) |
|-------------------------------|-------------------------|------------------|---|-----------------------------|--|--|--|------------------------------|
| 66 ATr 39 <sup>1</sup>        | Qtz <sup>+</sup> lusSch | muscovite        | 9.80                                    | 183.4                       |  |  | .91  | 122 $\pm$ 3.7                |
|                               |                         |                  | 9.90                                    |                             |  |  |  |                              |
|                               |                         |                  | $\bar{x} = 9.85$                        |                             |  |  |  |                              |
| 66 APa 129 <sup>2</sup>       | Tuff                    | biotite          | 7.05                                    | 88.76                       |  |  | .94  | 83.4 $\pm$ 2.2               |
|                               |                         |                  | 7.05                                    |                             |  |  |  |                              |
|                               |                         |                  | $\bar{x} = 7.05$                        |                             |  |  |  |                              |
| 66 APa 131 <sup>1</sup>       | Qtz <sup>+</sup> lusSch | muscovite        | 10.12                                   | 167.1                       |  |  | .95  | 108.5 $\pm$ 3.3              |
|                               |                         |                  | 10.13                                   |                             |  |  |  |                              |
|                               |                         |                  | $\bar{x} = 10.125$                      |                             |  |  |  |                              |
| 66 APa 44 <sup>3</sup>        | Meta-Granite            | hornblende       | .743                                    | 13.90                       |  |  | .93  | 121 $\pm$ 3.8                |
|                               |                         |                  | .758                                    |                             |  |  |  |                              |
|                               |                         |                  | $\bar{x} = .751$                        |                             |  |  |  |                              |
| 62 ABe 264 <sup>4</sup>       | Meta-Granite            | biotite          | 8.85                                    | .0471                       |  | 5.25   | .94  | 88 $\pm$ 4                   |
| 62 ABe 264 <sup>4</sup>       | Meta-Granite            | muscovite        | 10.30                                   | .0573                       |  | 5.49   | .96  | 92 $\pm$ 5                   |
| 62 ARr 192 <sup>4</sup>       | Meta-Granite            | biotite          | 9.10                                    | .0475                       |  | 5.15   | .96  | 86 $\pm$ 4                   |
| 60 ATr 134 <sup>5</sup>       | Meta-Granite            | muscovite        | 10.52                                   | 157.6                       |  |  | .91  | 98.8 $\pm$ 2.2               |
|                               |                         |                  | 10.52                                   |                             |  |  |  |                              |
|                               |                         |                  | $\bar{x} = 10.52$                       |                             |  |  |  |                              |

<sup>1</sup>Mayfield, C. F., 1975, Metamorphism in the southwestern Brooks Range: Geological Survey Research 1975, U.S. Geol. Survey Professional Paper 975, p. 64-65.

<sup>2</sup>Patton, W. W., Jr., and Miller, T. P., 1968, Regional geologic map of the Selawik and southern Baird Mountains quadrangles, Alaska: U.S. Geol. Survey Map I-530, 1 sheet.

<sup>3</sup>Patton, W. W., Jr., Miller, T. P., and Tailleir, I. L., 1968, Regional geologic map of the Shungnak and southern part of the Ambler River quadrangles, Alaska: U.S. Geol. Survey, 1 sheet.

<sup>4</sup>Grosge, W. P., and Reiser, H. N., 1971, Preliminary bedrock geologic map Wiseman and eastern Survey Pass quadrangles, Alaska: U.S. Geol. Survey Open-File Rep. 479, 2 sheets.

<sup>5</sup>Pessel, G. H., Garland, R. E., Tailleir, I. L., and Eakins, G. R., 1973, Preliminary geologic map of southeastern Ambler River and part of Survey Pass quadrangles, Alaska: Alaska State Division of Geological Surveys, Open-File Report 28, 1:63,360, 2 sheets.